Measurements and modeling of water transport and osmoregulation in a single kidney cell using optical tweezers and videomicroscopy

A. D. Lúcio,[1] R. A. S. Santos,[2] and O. N. Mesquita[1,*]
[1]*Departamento de Física, ICEX, Universidade Federal de Minas Gerais, Caixa Postal 702, Belo Horizonte, CEP 30123-970 Minas Gerais, Brazil*
[2]*Departamento de Fisiologia e Biofísica, ICB, Universidade Federal de Minas Gerais, Belo Horizonte, CEP 30123-970 Minas Gerais, Brazil*
(Received 30 May 2003; published 10 October 2003)

With an optical tweezer installed in our optical microscope we grab a single Madin Darby Canine kidney cell and keep it suspended in the medium without touching the glass substrate or other cells. Since the optically trapped cell remains with a closely round shape, we can directly measure its volume by using videomicroscopy with digital image analysis. We submit this cell to a hyperosmotic shock (up-shock) and video record the process: the cell initially shrinks due to osmotic efflux of water and after a while, due to regulatory volume increase (RVI), an osmoregulation response, it inflates again (water influx) until it reaches a new volume (the regulatory volume V_R). In addition to considering standard osmotic water transport, we model RVI using a simple phenomenological model. We obtain an expression for cell volume variation as a function of time that fits very well with our experimental data, where two characteristic times appear naturally: one related to water transport and the other related to RVI. From the fit we obtain water permeability, osmolyte influx rate for RVI, and regulatory volume. With the addition of the hormone vasopressin, water permeability increases while the regulatory volume decreases until inhibition of RVI. In summary, we present a technique to measure directly volume changes of a single isolated kidney cell under osmotic shock and a phenomenological analysis of water transport that takes into account osmoregulation.

DOI: 10.1103/PhysRevE.68.041906 PACS number(s): 87.16.Dg, 87.64.−t, 87.80.Cc, 89.40.Cc

I. INTRODUCTION

Pure lipid biological membranes are poorly permeable to water (10^{-5}–10^{-4} cm/s), while water permeability of plasma membranes of epithelial cells involved in fluid transport can be much higher (10^{-3}–10^{-1} cm/s) [1]. This observation led to the identification of a family of molecular water channels (aquaporins) that mediate and regulate water transport across plasma membranes [2,3]. In order to determine whether water channels can account quantitatively for the water permeability observed in epithelial cell plasma membranes, several model systems and different techniques have recently been developed to measure water permeability [4–8]. Water transport is ubiquitous in cells; therefore the technique described here is of general applicability in cell biology. In particular, precise measurements of water permeability in kidney cells are important as part of the understanding of renal disorders, hypertension, and how drugs can affect them. The central idea of most experiments is to submit layer of cells or tissues to an osmotic up- or down-shock and measure variation of cell volume as a function of time. From the fit of the data to some model function one can obtain water permeability [4]. The main difference between the various techniques is how cell volume change as a function of time is measured. The experiments carried out to now were performed on layers of kidney cells or on tissues and used light interference, fluorescence, and other optical techniques where assumptions about the shape of the cells have to be made in order to obtain the variation of cell volume [4–8]. To circumvent such problems and have a completely isolated cell we use an optical tweezer that consists of a single laser beam focused by a high numerical aperture objective (1.4) that can trap dielectric particles near its focus [9–11]. With an optical tweezer installed in our microscope (see Fig. 1) we grab a single Madin Darby Canine Kidney (MDCK) cell [12,13] and keep it suspended in the medium without touching the glass substrate or other cells. The optically trapped cell remains with a closely round shape, such that we can directly measure its volume by using videomicroscopy with digital image analysis. We submit this cell to a hyperosmotic shock (up-shock) and video record the process: the cell initially shrinks (see Fig. 2) and after a while, due to osmoregulation, there is a reuptake of water [regularly volume increase (RVI)], and the cell inflates again until it reaches a new volume (regulatory volume V_R). A plot of the time evolution of the normalized volume of a single MDCK cell after an osmotic up-shock of 200 mOsm—change in external osmolarity from 300 to 500 mOsm—is shown in Fig. 3. The response time for equilibration of the external osmolarity around the cell in our chamber is of the order of 1–2 s. The final external osmolarity is kept constant due to continuous circulation of the medium with the new osmolarity through the chamber with the cell. Our data in Fig. 3 cannot be fitted by the standard model that has been used in most of the analysis in the literature up to now [4–8], since the standard model only takes into account passive osmotic water transport and not uphill water transport that leads to RVI as clearly shown in our data. The standard model predicts, for our experimental conditions, a single decaying ex-

*Author to whom correspondence should be addressed. Email address: mesquita@fisica.ufmg.br

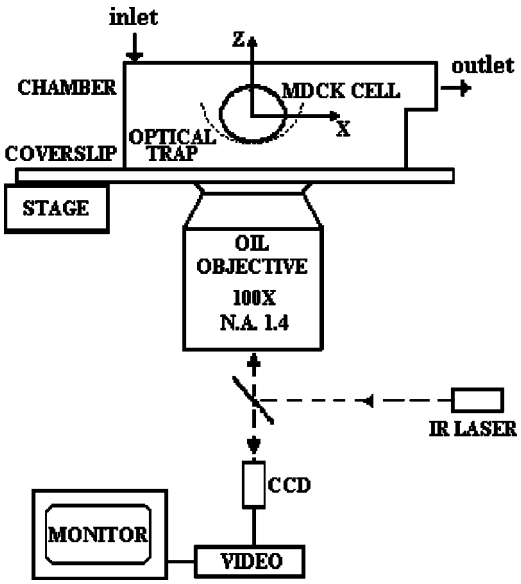

FIG. 1. Setup. The optical tweezer is mounted on a Nikon TE300 Eclipse Microscope and consists of an IR laser beam from a diode-laser SDL-5280 that goes through an oil objective and trap cells near the objective focus. Visualization is accomplished with the same objective and a charge-coupled device camera (DAGE MTI). Images are recorded with a videocassette recorder (EVO 9650 SONY). Later, images are digitized with a frame grabber (Data Translation), stored in a PowerPC microcomputer, and processed using the program NIH IMAGE. Our chamber allows a continuous flow of the medium solution.

ponential function, for the variation of volume as a function of time, which is incompatible with our experimental data. Electrophysiological studies of MDCK cells after osmotic up-shocks have been done in an attempt to identify the microscopic mechanisms responsible for RVI. A sudden exposure of MDCK cells to hypertonic extracellular fluids leads to an increase of the cell membrane K^+ selectivity, paralleled by a marked decrease of cell membrane conductance involving both K^+ and Cl^- conductances. The reduction of cell membrane conductances tends to reduce cellular loss of ions and is supportive of RVI. However, the accumulation of ions required by RVI cannot be achieved by inhibition of ion conductance alone but must involve mechanisms increasing cell osmolarity [14]. More recently, an electron microprobe analysis indicates a pronounced increase of K, Cl, and Na

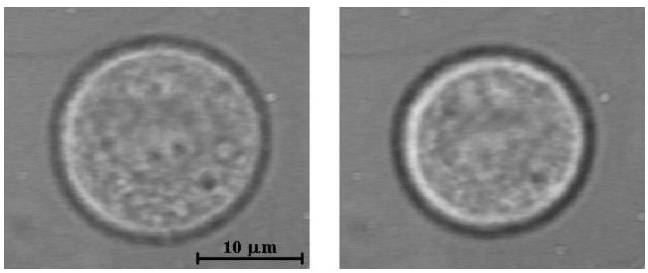

FIG. 2. Left: Bright-field image of an optically trapped MDCK cell in equilibrium in a medium of 300 mOsm. Right: Image of the same cell 15 s after a hyperosmotic shock of 200 mOsm.

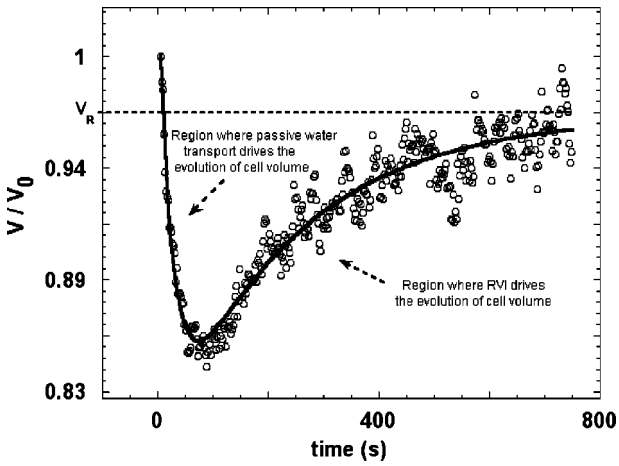

FIG. 3. Time evolution of the normalized volume of the single MDCK cell of Fig. 1, under osmotic up-shock from 300 mOsm to 500 mOsm. Circles are the experimental points and continuous curve is the fit using Eq. (13). The fit returns $P=6.6\pm0.3$ μm/s, $\alpha=(8.5\pm0.4)\times10^{-10}$ mol/s cm^2, $V_R/V_0=0.95\pm0.04$, and $b/V_0=0.52\pm0.02$.

contents in MDCK cells during RVI after a hyperosmotic stress. However, the long term volume regulation in MDCK cells is achieved by osmolytes not detectable by electron microprobe analysis [15]. A complete set of microscopic mechanisms to explain RVI in MDCK cells is still lacking. A discussion of general models for water transport with RVI across leaky epithelia can be found in the paper by Zeuthen [16] and for bacterial cells in the paper by Csonka and Epstein [17]. In this paper we propose a simplified phenomenological model of transport where all microscopic mechanisms for RVI are lumped into a single constant α that introduces a new time scale into the problem. Our model fits very well with our experimental data, and in addition to water permeability we can obtain the constant α and the regulatory volume V_R. This seems to be a good way of quantitatively characterizing RVI in our system and may be useful for deciding among the main microscopic mechanisms for RVI. Measurements can also be done in the presence of drugs. One can use our model to determine how RVI is affected by such drugs. An example will be provided from an up-shock in MCDK cells treated with the antidiuretic hormone vasopressin. Our model provides one step beyond the standard analysis of water transport in cells by including a simple phenomenological model of RVI, which fits very well with our experimental data for MDCK cells. Therefore, we have a good experimental model system, since it consists of a well-known kidney cell (MDCK), completely isolated from the substrate and from other cells, and a technique that returns direct measurements of cell volume as a function of time.

II. MATERIALS AND METHODS

A. Cell culture and loading

MDCK cells (provided by Dulce Cazarine-UNIFESP), passages 28–35, are grown in cell culture flasks (by Nalge

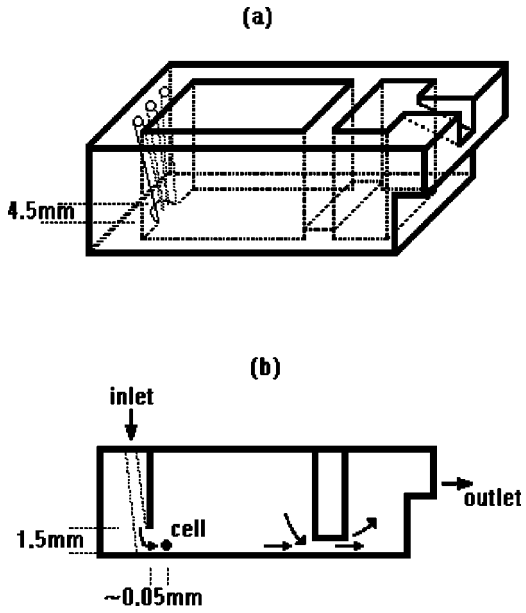

FIG. 4. Flow chamber.

Nunc International) in D-MEM/F-12 medium (GIBCO) containing 1mM HEPS and 10 ml antibiotic-antimycotic (GIBCO) supplemented with 10% fetal calf serum at 37 °C in 5% CO_2 atmosphere. The cell culture medium was exchanged three times per week. MDCK cells were used at 50–70 % confluence. Cells grown to confluence were lift off the culture chamber by tripsinization; cells were washed with phosphate-buffered saline (PBS - GIBCO BRL) and exposed to 0.2-ml trypsin solution (0.25% flesh trypsin and 0.03% EDTA) in 0.4-ml PBS, $p\mathrm{H}=7.2$ for 4 m. Isolated cells were suspended and 50% of the solution was immediately transferred to 5-ml cell culture medium containing, 0, 18, 36, or 54 mM of AVP (Arg^8 vasopressin—Bachem); the 50% remainder was transferred to a new cell culture flask containing 5 ml of cell culture medium. Cell culture medium (500 mOsm) containing 0-, 18-, 36-, or 54-mM AVP was used for hyperosmotic perfusion. This solution was prepared with D-MEM/F-12 medium adjusted to 500 mOsm by addition of 100-mM NaCl.

B. Flow chamber

Details of our flow chamber are shown in Fig. 4. The chamber is composed of two sections to minimize fluctuations in the region where the cell under study is located. The chamber contains the cell in equilibrium with its medium. The ability to measure the permeability with accuracy depends on the response time for equilibration of the system to a new osmolarity after the osmotic shock. To have the fastest possible response time for equilibration of the osmolarity around the cell, the cell grabbed by the optical tweezers is put around 50 μm from the flow entrance and as close as possible from the bottom of the chamber. The flow rate is adjusted to maximum before the cell pops out from the tweezers. From the time we turn the flow with the medium with a new osmolarity until the cell starts to shrink it takes 1–2 s. Since the kidney cell used is much smaller than the flow inlet area (1.5×4.5 mm^2), the osmolarity around the cell equilibrates very rapidly to the nominal value of the osmolarity of the flow-in solution, even though the osmolarity in the whole flow chamber is highly nonuniform. An estimate for the equilibration time around the cell can be done by (equilibration time)=(diameter of the cell)/(flow velocity) $\approx 20\ \mu\mathrm{m}/25\ \mu\mathrm{m/s}\sim 1$ s. Since the fast decay times measured are around 15 s, we are in fact measuring cell permeability which are little affected by the equilibration time around the cell.

C. Optical tweezers and videomicroscopy setup

We use a Nikon TE300 microscope with an oil immersion microscope objective with magnification of 100× and numerical aperture 1.4, in a bright field configuration. Measurements were performed at 25 °C. Visualization is made with the same objective and recorded with a digital camera (DAGE MTI) and a videocassette recorder (EVO 9650-SONY). The optical tweezers consists of a collimated beam of infrared laser (SDL 5280) that goes through the objective. The influence of the optical tweezer IR laser on the cell, up to the local power of 20 mW, was checked using Trypan Blue. Until 2 h of cell exposition to the laser, no apparent damage was observed. Details of our experimental setup can be obtained from Viana *et al.* [11].

D. Image analysis

Recorded images were digitized as movies with 8-bit graylevels, using a Data Translation frame grabber and stored in a PowerPC microcomputer. The movies of the cells under osmotic shock were analyzed with the program NIH IMAGEJ. The program extracts the cell area and then the volume is obtained.

III. MODEL OF WATER TRANSPORT WITH OSMOREGULATION

For an osmotic up-shock the cell volume initially decreases due to outflow of water. In the previous studies, RVI was not taken into account such that the initial cell volume variation as a function of time was fit to a single exponential function whose decay time is related to water permeability [4–8]. If, however, the cell volume is left to evolve for a longer time, like in Fig. 3, the cell inflates due to reuptake of water (RVI). As mentioned before, RVI in MDCK cells can be caused by the uptake of several osmolytes after the hyperosmotic shock, but a clear picture of all mechanisms leading to RVI is still lacking. Our model contains the standard term for passive osmotic water transport plus a term related to RVI, as described below.

Let us assume that the water permeability P(cm/s) for a given plasmatic membrane is constant during an osmotic shock. Using Fick's law and the difference in osmotic pressures between intra cellular and extracellular regions, the variation of the mass of water M_w (mol) inside the cell can be written as

$$\frac{dM_w}{dt}=A_0P(\phi_i-\phi_e), \tag{1}$$

where ϕ_i is the internal cell osmolarity (moles/cm^3), ϕ_e is the external cell osmolarity (moles/cm^3), A_0 is the initial membrane area (cm^2), and P is water permeability (cm/s). If ϕ_i is larger than ϕ_e water flows into the cell increasing M_w, whereas in the opposite case water flows out the cell. The total cell volume V is not completely occupied by water. If b is the osmotically inactive volume (cm^3) [4], the volume occupied by water that is osmotically active is V-b. It is important to emphasize that the area A_0 is the total membrane area assumed constant during the osmotic shock and not the cell area. This assumption implies that the total number of pores active for water transport remains constant during the osmotic shock [4]. Therefore, we can rewrite the equation above to obtain

$$\frac{d(V-b)}{dt}=\frac{A_0P}{\rho_w}\left[\frac{M_s}{V-b}-\phi_e\right], \tag{2}$$

where ρ_w is the water density (1/18 mol/cm^3) and M_s is the total osmolyte mass (mol) in the osmotically active regions. Solving Eq. (2) for an osmotic up-shock and for small variations of volume, and keeping M_s constant, leads to the standard single exponential decaying function for the volume of the cell as a function of time as obtained by Farinas *et al.* [4,6]. We model osmolyte transport for RVI by allowing the variation of M_s following the equation below

$$\frac{dM_s}{dt}=-\alpha A_0\left(\frac{V-V_R}{V_0}\right), \tag{3}$$

where V_R is the regulatory volume (cm$_3$) and α is a constant related to the rate of osmolyte transport for RVI per unit area of the membrane (mol/s cm^2); α may be different for an up or down osmotic shock. Our proposal then is that the rate of osmolyte influx towards regions osmotically active inside the cell is proportional to the relative deviation of the volume of the cell in relation to the final volume V_R. The cell may return to the initial volume V_0, but in general it returns to a final equilibrium volume V_R that is close to V_0. V_R is the new equilibrium volume after the osmotic shock and RVI, consequently it is independent of our model. After some simple mathematical manipulation, Eqs. (2) and (3) result in a nonlinear second-order differential equation for the time evolution of cell volume given by

$$\frac{1}{2}\frac{d^2(V-b)^2}{dt^2}+\gamma_1\frac{d(V-b)}{dt}+\gamma_2(V-b)=\gamma_2(V_R-b), \tag{4}$$

where

$$\gamma_1=\frac{P_wA_0\phi_e}{\rho_w} \tag{5}$$

and

$$\gamma_2=\frac{P_wA_0^2\alpha}{\rho_wV_0}. \tag{6}$$

For small volume variations ΔV, we have

$$(V-b)=(V_0-b)+\Delta V, \tag{7}$$

where V_0 is the initial cell volume (cm^3) and $\Delta V \ll (V_0-b)$. Then Eq. 4 can be linearized and written as

$$\frac{d^2\Delta V}{dt^2}+\frac{\gamma_1}{(V_0-b)}\frac{d\Delta V}{dt}+\frac{\gamma_2}{(V_0-b)}\Delta V=\frac{\gamma_2}{(V_0-b)}(V_R-V_0). \tag{8}$$

Equation (8) is a differential equation of a single damped harmonic oscillator, with two characteristic time scales:

$$\tau_1=\left[\frac{\gamma_1}{2(V_0-b)}+\frac{1}{2}\sqrt{\left(\frac{\gamma_1}{(V_0-b)}\right)^2-\frac{4\gamma_2}{(V_0-b)}}\right]^{-1} \tag{9}$$

and

$$\tau_2=\left[\frac{\gamma_1}{2(V_0-b)}-\frac{1}{2}\sqrt{\left(\frac{\gamma_1}{(V_0-b)}\right)^2-\frac{4\gamma_2}{(V_0-b)}}\right]^{-1}. \tag{10}$$

For the initial conditions ($t=0$),

$$\Delta V=0, \tag{11}$$

$$\phi_i-\phi_2=-\Delta\phi_0, \tag{12}$$

where $\Delta\phi_0$ is the osmotic shock (mol/cm^3) considered positive for an up-shock like in our experiments and using Eqs. (8)–(10) an expression for the cell volume $V(t)$ as a function of time predicted by our model is given by

$$V(t)=Ae^{-t/\tau_1}-Be^{-t/\tau_2}+V_R, \tag{13}$$

where

$$A=\frac{\tau_1\tau_2}{\tau_2-\tau_1}\frac{P_wA_0\Delta\phi_0}{\rho_w}+\frac{\tau_1(V_R-V_0)}{\tau_2-\tau_1} \tag{14}$$

and

$$B=\frac{\tau_1\tau_2}{\tau_2-\tau_1}\frac{P_wA_0\Delta\phi_0}{\rho_w}+\frac{\tau_2(V_R-V_0)}{\tau_2-\tau_1}. \tag{15}$$

If $\gamma_1^2 \gg 4.\gamma_2.(V_0-b)$, then $\tau_2 \gg \tau_1$, a condition that is usually satisfied by our experimental data, a simplified final equation is obtained with a simpler interpretation of the two characteristic times, namely,

$$A=\frac{(V_0-b)\Delta\phi_0}{\phi_e}, \tag{16}$$

$$B=\frac{(V_0-b)\Delta\phi_0}{\phi_e}+(V_R-V_0), \tag{17}$$

$$\tau_1=\frac{\rho_w(V_0-b)}{P_wA_0\phi_e}, \tag{18}$$

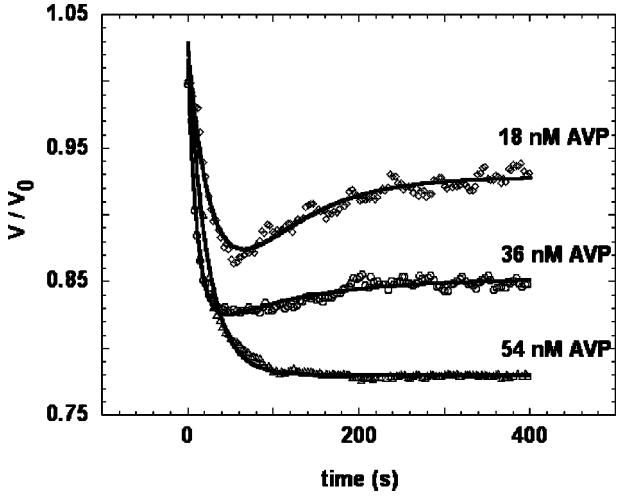

FIG. 5. Time evolution of the normalized volume of trapped MDCK cells under an osmotic up-shock from 300 mOsm to 500 mOsm: lozenges are the data for vasopressin concentration of 18 nM, circles for 36 nM and triangles for 54 nM. Continuous curves are the fits using Eq. (13).

$$\tau_2 = \frac{\phi_e V_0}{\alpha A_0}. \tag{19}$$

In this approximation the fast time constant τ_1 is associated with water transport while the slow time constant τ_2 is associated with osmolyte transport for RVI. If we neglect RVI ($\tau_2 = \infty$), the simplified expressions above for A and τ_1 [Eqs. (16) and (18)] are those used by Farinas *et al.* [4] to fit with their data. The same expression has since then been used by all the other authors. Therefore our model is a generalization of previous models.

IV. EXPERIMENTS AND DISCUSSIONS

Equation (13) fits very well with our experimental data, as shown in Figs. 3 and 5. We use a nonlinear square fitting routine to fit the data. From the fit, we obtain the parameters τ_1, τ_2, A, B, and V_R, and using Eqs. (14) and (15) we obtain the values for the water permeability, osmolyte influx rate, regulatory volume, and the volume osmotically inactive. For the data of Fig. 3, this fit returns $P = 6.6 \pm 0.3$ μm/s, $\alpha = (8.5 \pm 0.4) \times 10^{-10}$ mol/s cm^2, $V_R/V_0 = 0.95 \pm 0.04$, and $b/V_0 = 0.52 \pm 0.02$. Values obtained by Zelenina *et al.* [7] are $P = 2.73 \pm 0.26$ μm/s and $b/V_0 = 0.57 \pm 0.04$, by Farinas *et al.* [6] from $P = 9 \pm 4$ μm/s up to $P = 24 \pm 7$ μm/s, depending on which side of the cell in the monolayer (apical or basolateral) the measurement is performed, a distinction that we cannot make since we are measuring a single isolated cell. Since Zelenina *et al.* and Farinas *et al.* did not investigate RVI, they did not measure either α or V_R.

We also performed experiments with the addition of the antidiuretic hormone vasopressin. Vasopressin is known to activate a metabolic path that translocates aquaporins-2 from an intracellular compartment to the apical membrane, increasing the membrane number of pores and consequently increasing its water permeability [18–21]. Data in Fig. 5 was obtained after the addition of 18, 36, and 54 nM of vasopressin. Concentrations of vasopressin are kept constant during the experiments since the medium with such concentrations circulates continuously through the chamber. Equation (13) also fits very well with the data with vasopressin as shown in Fig. 5. We observe that water permeability increases while regulatory volume decreases, a parameter that has not been measured before. We observe also that with addition of vasopressin cells become structurally weaker and there is a greater chance of membrane ruptures occurring. A summary of the results is shown in Table I.

TABLE I. NR—No or very slow RVI that could not be measured for an experimental run time of around 10 min. Averages were made over measurements from ten different cells for AVP concentrations of zero and 54 nM and from five different cells for the other concentrations. The error bars correspond to the standard deviations.

AVP (nM)	α (10^{-10} mol/s cm^2)	V_R (%V_0)	P (μm/s)	b (%V_0)
0	8.0 ± 1.5	94 ± 6	5.2 ± 2.1	63 ± 6
18	6.1 ± 5.2	90 ± 3	9.4 ± 3.5	56 ± 15
36	13 ± 3	85 ± 3	15.1 ± 4.5	68 ± 4
54	NR	NR	16.6 ± 6.1	57 ± 12

V. CONCLUSIONS

In conclusion, we presented a technique based on optical tweezing and videomicroscopy that allows us to follow directly the time evolution of the volume of a single isolated kidney cell under osmotic up-shock. In addition to osmotic water transport, we introduced a phenomenological term that takes into account RVI. In our simplified model the mechanisms of RVI are lumped into a single constant α that introduces a new time scale into the problem. The model fits very well with the experimental data, indicating that just two time constants are sufficient to explain the observed transport: one time constant associated with water transport and the other time constant associated to osmolyte transport. In addition to water permeability, novel parameters, such as osmoregulation, osmolyte influx rate, and regulatory volume were measured which might be useful for understanding the mechanisms of RVI and the behavior of kidney cells and of other cells in the presence of hormones and drugs.

ACKNOWLEDGMENTS

We acknowledge the Brazilian agencies: Fapemig, CNPq, Finep-Pronex, and Instituto do Milênio de Nanociência-MCT.

[1] M.L. Zeidel, Semin Nephrol. **18**, 167 (1998).
[2] P. Agre, J. Am. Soc. Nephrol. Apr **11**, 764 (2000).
[3] S. Verkman and K. Mitra, Am. J. Physiol. Renal Physiol. **278**, F13 (2000).
[4] J. Farinas, V. Simanek, and A.S. Verkman, Biophys. J. **68**, 1613 (1995).
[5] M.M. Timbs and K.R. Spring, J. Membr. Biol. **153**, 1 (1996).
[6] J. Farinas, M. Kneen, M. Moore, and A.S. Verkman, J. Gen. Physiol. **10**, 283 (1997).
[7] M. Zelenina and H. Brismar, Eur. Biophys. J. **29**, 165 (2000).
[8] K. Maric, B. Wiesner, D. Lorenz, E. Klussmann, and W. Rosenthal, Biophys. J. **80**, 1783 (2001).
[9] A. Ashkin and J.M. Dziedzic, Science **235**, 1517 (1987).
[10] K. Svoboda and S.M. Block, Annu. Rev. Biophys. Biomol. Struct. **23**, 247 (1994).
[11] N.B. Viana, R.T.S. Freire, and O.N. Mesquita, Phys. Rev. E **65**, 041921 (2002).
[12] S.R. Gaush, W.L. Hard, and T.F. Smith, Proc. Soc. Exp. Biol. Med. **122**, 931 (1966).
[13] M.H. Saier, Jr., Am Physiol Soc. **240**, C106 (1981).
[14] M. Ritter, M. Steidl, and F. Lang, Am. J. Physiol. **261**, C602 (1991).
[15] S. Borgmann and A. Dörge, Kidney Int., Suppl. **67**, S-133 (1998).
[16] T. Zeuthen, Int. Rev. Cytol. **215**, 285 (2002).
[17] L.N. Csonka and W. Epstein, *Escherichia coli and Salmonella: Cellular and Molecular Biology*, edited by Frederick C. Neidhardt (ASM Press, Washington, D.C., 1996), Vol. 1, pp. 1210–1223.
[18] S. Nielsen, C-L. Chou, D. Marples, E.I. Christensen, B.K. Kishore, and M.A. Knepper, Proc. Natl. Acad. Sci. U.S.A. **92**, 1013 (1995).
[19] P.M.T. Deen, J.P.L. Rijss, S.M. Mulders, R.J. Errington, J. VanBaal, and C.H. Vanos, J. Am. Soc. Nephrol. **8**, 1493 (1997).
[20] D.T. Ward, T.G. Hammond, and H.W. Harris, Annu. Rev. Physiol. **61**, 683 (1999).
[21] M.M. Aires, *Fisiologia* (Guanabara Koogan S. A., Rio de Janeiro, 1999).